Materials Science & Engineering A 685 (2017) 244–252

Contents lists available at ScienceDirect

Materials Science & Engineering A

journal homepage: www.elsevier.com/locate/msea

Effect of pre-homogenization deformation treatment on the workability and mechanical properties of AlMg5Si2Mn alloy

Yun-Soo Lee[a], Joon-Hyeon Cha[a,b], Su-Hyeon Kim[a,*], Cha-Yong Lim[a], Hyoung-Wook Kim[a,c]

[a] Metallic Materials Division, Korea Institute of Materials Science, Changwon 51508, Republic of Korea
[b] Department of Materials Science and Engineering, Pusan National University, Busan 46241, Republic of Korea
[c] Department of Advanced Materials Engineering, Korea University of Science and Technology, Daejeon 34113, Republic of Korea

ARTICLE INFO

Keywords:
Aluminum alloy
Homogenization
Microstructure
Mg_2Si
Workability
Mechanical properties

ABSTRACT

This study evaluated the effect of a novel treatment method on the potential application of AlMg5Si2Mn die casting alloy as a substitute for wrought aluminum alloy in products. The proposed pre-homogenization deformation treatment was intended to increase the hot workability of the AlMg5Si2Mn alloy, which is typically not malleable due to the presence of interconnected brittle phases. By disintegrating interconnected eutectic Mg_2Si phases into fragmented particles, the slight cold rolling before homogenization significantly enhanced hot rolling workability. Rolled sheets were successfully fabricated by hot and subsequent cold rolling, and the sheets exhibited enhanced mechanical properties compared to cast samples.

1. Introduction

Aluminum alloys have been widely utilized in the transportation industry, due to their high strength-to-weight ratio, good environmental resistance, and excellent recyclability. Over the past few decades, aluminum alloys have become increasingly popular in automotive applications, because they are an effective alternative to steels, while providing weight-savings, resulting in improved automobile fuel efficiency [1,2]. Various kinds of aluminum alloys are used in car parts, and aluminum alloy scraps from cars are valuable materials in recycling industries. It is well known that aluminum recycling uses only 5% of the energy needed to make the same amount of aluminum from bauxite ore [3]. However, unlike beverage cans, car parts scraps are not readily recyclable into the same quality of products, because of the variety of alloy compositions. Casting and wrought products have distinctive and valuable differences in composition [4], but they become low grade scraps when they are mixed together for recycling. Most cast alloys contain high levels of alloying elements such as silicon, typically ranging from 3 to 30 wt%. Wrought products, however, only contain 1.5 wt% or less silicon. Al-Mg-Si alloys can be used for both cast and wrought products depending on the relative content of magnesium and silicon. Al-Mg-Si alloys contain more than 3 wt% of magnesium and 0.3 wt% of silicon when they are used for casting products, but wrought Al-Mg-Si alloys typically have 1 wt% of magnesium.

AlMg5Si2Mn is a high pressure die casting (HPDC) alloy which has a good combination of strengths and elongation [5,6]. Casting products of this alloy are appropriate for use as structural parts in automobile car bodies and chassis. However, AlMg5Si2Mn is not considered appropriate for wrought products due to the presence of interconnected Mg_2Si phases, and therefore there has been no report on the deformation characteristics of this alloy. A car body is made of many different kinds of casting and wrought components, and sometimes they are joined together. For these reasons, multiple benefits can be expected during manufacturing, application and recycling if the casting and wrought aluminum alloy products have the same composition.

The Al-Mg-Si cast alloys, such as AlMg5Si2Mn alloy, mainly contain α(Al) dendrites, primary Mg_2Si particles and/or eutectic α(Al)+Mg_2Si phases. A major issue regarding Al-Mg-Si cast alloys is to modify primary and eutectic Mg_2Si phases to more fine, equiaxed, and uniformly distributed, in order to improve mechanical response of the alloys [7–15]. Numerous studies on the modification of Mg_2Si phases have been reported, focusing on the effect of heat treatment and addition of modifying agents. Al-Mg-Si cast alloys are conventionally heat treated at high temperature, close to the eutectic temperature of the alloys [7–9]. Heat treatment can homogenize the microstructure by re-distributing the alloying elements, dissolve the soluble phases containing Mg and Si into the matrix, and spheroidize the Mg_2Si phases by atomic diffusion. Another feasible method is chemical modification by using modifying agents [10–13]. Morphology of primary and eutectic Mg_2Si phases in Al-Mg-Si cast alloys can be changed by adding chemical modifiers such as Sr [10,11], P [10,12],

* Corresponding author.
E-mail address: shawnkim@kims.re.kr (S.-H. Kim).

http://dx.doi.org/10.1016/j.msea.2016.12.107
Received 5 September 2016; Received in revised form 23 December 2016; Accepted 23 December 2016
Available online 24 December 2016

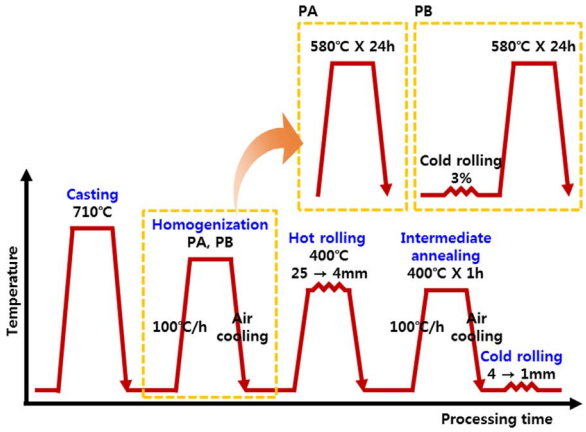

Fig. 1. Flow chart of the fabrication of AlMg5Si2Mn alloy sheets using different homogenization methods.

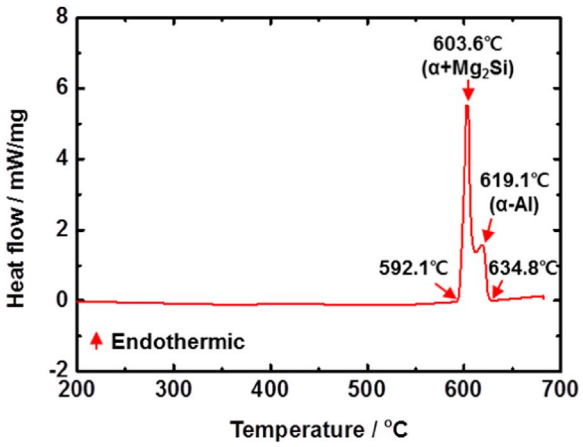

Fig. 2. DSC heating curve of the as-cast AlMg5Si2Mn alloy.

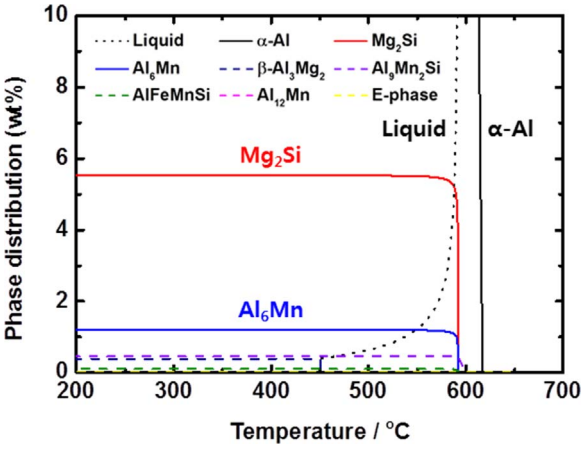

Fig. 3. Thermodynamically predicted mass fraction of the second phases during solidification of the AlMg5Si2Mn alloy.

and Ce [13]. It has been reported that the primary Mg_2Si particles can be modified by the following two mechanisms; one is heterogeneous nucleation, in which the modifying agents (or compounds formed by them) act as the heterogeneous nucleus, and the other is poisoning effect, in which the modifying agents absorb the forehead of growth and restrict the crystal growth [12]. Modification of the eutectic Mg_2Si by modifying agents is still a considerable controversy on the exact mechanisms [12,14]. Several possible mechanisms have been proposed based on the experimental results, for instance, the modification of the eutectic Mg_2Si phase is related to the effects of modifying agents on undercooling [10]. However, there are only a few reports dealing with the effect of plastic working on microstructure and mechanical properties of aluminum cast alloys [15]. It is because the aluminum cast alloys are not considered appropriate for wrought products.

The purpose of this study is to evaluate the potential application of the AlMg5Si2Mn HPDC alloy to wrought products. We especially focused on how plastic working prior to homogenization treatment affected workability. In addition, we addressed the possibility of fabricating rolled sheets of this proposed HPDC alloy, which was demonstrated to have enhanced mechanical properties compared to casting products.

2. Experimental procedures

The material used in this study was AlMg5Si2Mn HPDC alloy, which was prepared via an ingot metallurgical route. The fabrication flow chart, consisting of casting, homogenization, rolling, and heat treatment, is shown in Fig. 1. First, the alloy was melted in a graphite crucible using an electrical resistance furnace. The melt was held at 710 °C and then poured into a preheated copper mold to make slabs of 200 mm (width)×200 mm (height)×30 mm (thickness). The chemical composition of the alloy was measured by optical emission spectroscopy and is displayed in Table 1. Differential scanning calorimetry (DSC) was used to determine homogenization temperature. A coupon of 20 mg-weight was cut from the material and heated at 10 °C/min in a N_2 atmosphere in a PerkinElmer Pyris Diamond DSC. Solidification constituents were predicted using FactSage thermodynamic software under the non-equilibrium condition (Scheil-Gulliver cooling). The FTlite (FactSage light metal intermetallic compounds and alloy solutions) database was used for calculation. The X-ray diffraction (XRD, Rigaku D/MAX-2500V) analysis was carried out to identify the secondary phases using Cu-Kα radiation.

The cast slabs were handled with two different process routes. One method was heat treatment at 580 °C for 24 h (designated as PA), and the other was cold rolling to achieve 3% reduction, followed by heat treatment at 580 °C for 24 h (designated as PB). The homogenized slabs were then scalped to 25 mm thickness, preheated at 400 °C for 0.5 h, and hot rolled to 4 mm thickness. The hot rolled strips were annealed at 400 °C for 1 h, and further cold rolled to 1 mm thickness. The total reduction in thickness produced by hot and cold rolling was 96%. The rolled sheets were solution treated at 580 °C for 1 h followed by water quenching (T4). T4 samples were further heat treated at 250 °C for 1 h [6] to prepare T6 samples.

Optical microscopy (OM, Nikon Eclipse MA200) was employed to characterize the microstructures of as-cast, homogenized, and heat treated samples. A small coupon from the material was mounted in resin and the surface was mechanically polished. To observe grain structure, the polished surface was electro-chemically etched in a 5% fluoroboric acid solution. Image acquisition and analysis software (IMT i-Solution DT) was used to quantify the morphological characteristics

Table 1
Chemical composition of AlMg5Si2Mn alloy determined by optical emission spectroscopy (OES) analysis (mass fraction, wt%).

Element	Mg	Si	Mn	Fe	Cu	Zn	Ti	Al
Nominal [16]	5.0–6.0	1.8–2.6	0.5–0.8	≤0.20	≤0.05	≤0.07	≤0.20	bal.
OES	5.77	2.27	0.714	0.115	0.02	0.04	0.02	bal.

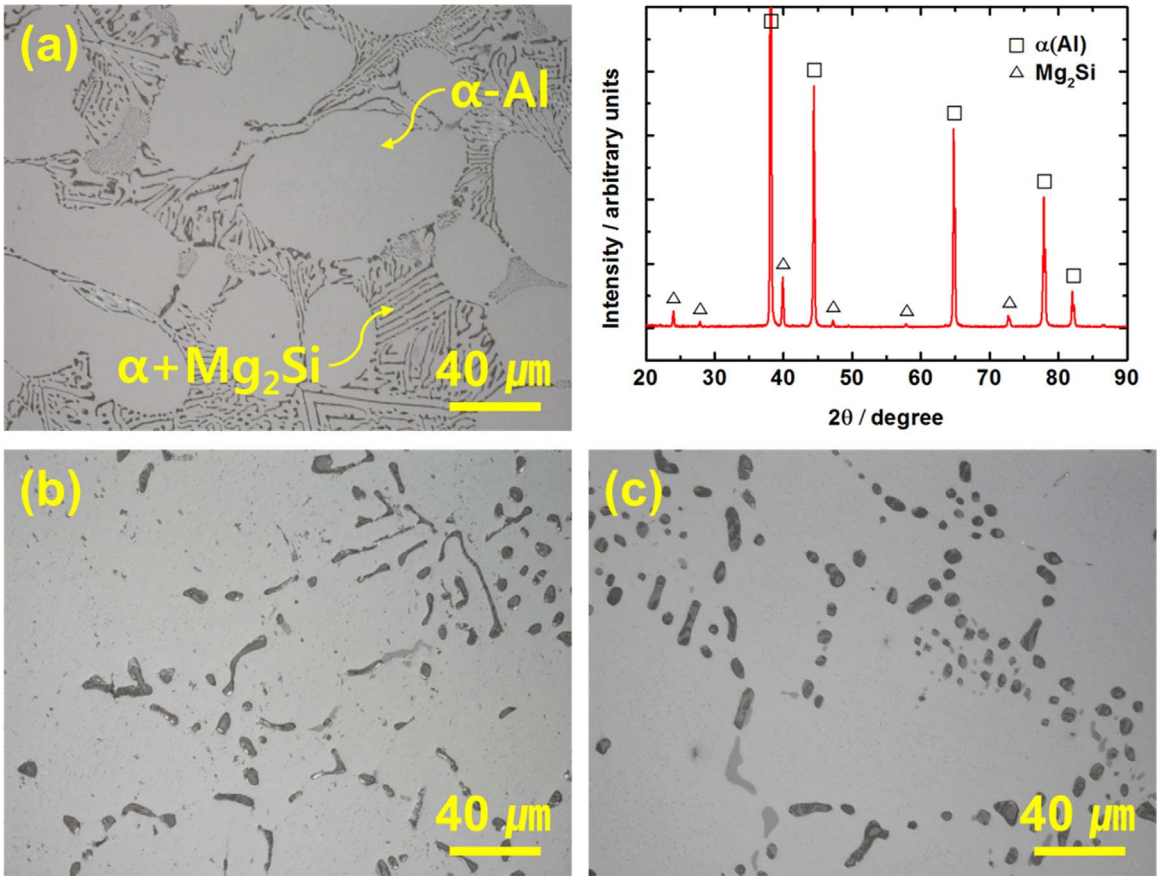

Fig. 4. Microstructures of (a) as-cast (with XRD results) and treated (b) PA, and (c) PB AlMg5Si2Mn alloy.

of the second phase particles, and to measure the grain size in the OM micrographs. A Robo-Met. 3D serial sectioning system [17] and Avizo Fire reconstruction software were used to obtain three-dimensional (3D) images of the second phases in as-cast and homogenized samples. The sample orientation was denoted with respect to RD (rolling direction), TD (transverse direction), and ND (normal direction). The microstructural analysis was performed on the TD sections unless otherwise noted. It is also noted that the RD is parallel to the casting direction (= gravity direction) of the samples.

Tensile tests were carried out with a universal testing machine (UTM, Instron 4206 and 5881) at ambient and elevated temperatures (300 and 400 °C). The specimens were machined from the homogenized slabs along the casting direction (=rolling direction, RD) with a diameter of 6 mm and a gauge length of 25 mm for high temperature tensile test according to ASTM E21-09. The crosshead speed during high temperature tensile tests was 0.125 and 1.5 mm/min before and after the yield point, respectively. The specimens for room temperature tensile test were machined from the sheets along the RD with a 25 mm gauge length according to ASTM E8/E8M-13a. The room temperature tensile tests were carried out with a crosshead speed of 1 mm/min.

3. Results and discussion

3.1. Effect of cold rolling prior to homogenization

The DSC curve of the as-cast AlMg5Si2Mn alloy is shown in Fig. 2. Two distinct endothermic peaks were found at 603.6 and 619.1 °C, which correspond to the melting of eutectic α(Al)+Mg_2Si and the bulk primary α(Al) dendrites, respectively, in good agreement with the thermodynamic calculations (Fig. 3). Based on these results, the optimum homogenization temperature was determined to be 580 °C.

Optical micrographs of the as-cast and homogenized samples are presented in Fig. 4. The as-solidified microstructure consisted of primary α(Al) dendrites and eutectic α(Al)+Mg_2Si, as shown in Fig. 4(a). In the eutectic region, a lamellar-like α(Al)+Mg_2Si structure with small amounts of blocky or rod-like Al_6Mn phase was observed [18]. The XRD result shows that the AlMg5Si2Mn alloy mainly contains α(Al) and Mg_2Si phases. Different microstructural morphologies were observed after homogenization: the Mg_2Si particles became coarse, disconnected, and/or spheroid, as shown in Fig. 4(b) and (c). In the PA treated sample, most of the eutectic Mg_2Si phases still exhibit a longish rod-like shape. Mg_2Si particles in the PB treated sample were more spheroidized than those in the PA treated sample, which means that cold rolling with small reductions prior to homogenization is a very effective method to spheroidize eutectic Mg_2Si particles.

Fig. 5 presents histograms of the length, diameter and aspect ratio of the Mg_2Si particles after PA and PB homogenization treatments. The geometrical parameters of Mg_2Si particles in the as-cast sample are also illustrated for comparison. Morphological differences in the Mg_2Si particles are clearly noted between the PA and PB treated samples. The PA treated samples exhibit bimodal distributions of particle size and aspect ratio, which means that there were two morphologies of Mg_2Si particles; one is characterized by small-sized and nearly spherical particles, and the other is coarse and rod-like. In contrast, PB treated samples had only small spheroid particles. It was confirmed that cold rolling prior to homogenization promoted the disconnection and spheroidization of eutectic Mg_2Si particles.

3D images of eutectic Mg_2Si phases in as-cast and homogenized samples are shown in Fig. 6. The as-cast samples exhibit lamellar structure of the eutectic Mg_2Si, as shown in Fig. 6(a). After homogenization, the eutectic Mg_2Si transformed to seaweed-like and coral-like morphologies as shown in Fig. 6(b) and (c), respectively. The 3D

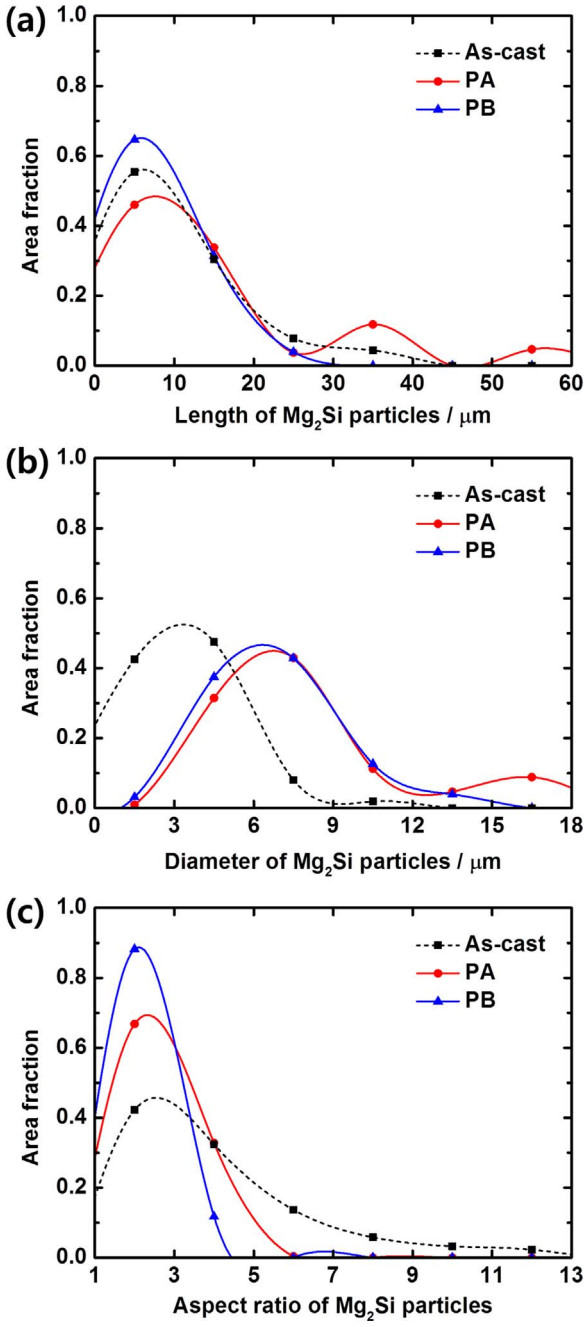

Fig. 5. Histograms for (a) length, (b) diameter and (c) aspect ratio of Mg_2Si particles in as-cast and homogenized AlMg5Si2Mn alloys, as obtained from 2D images.

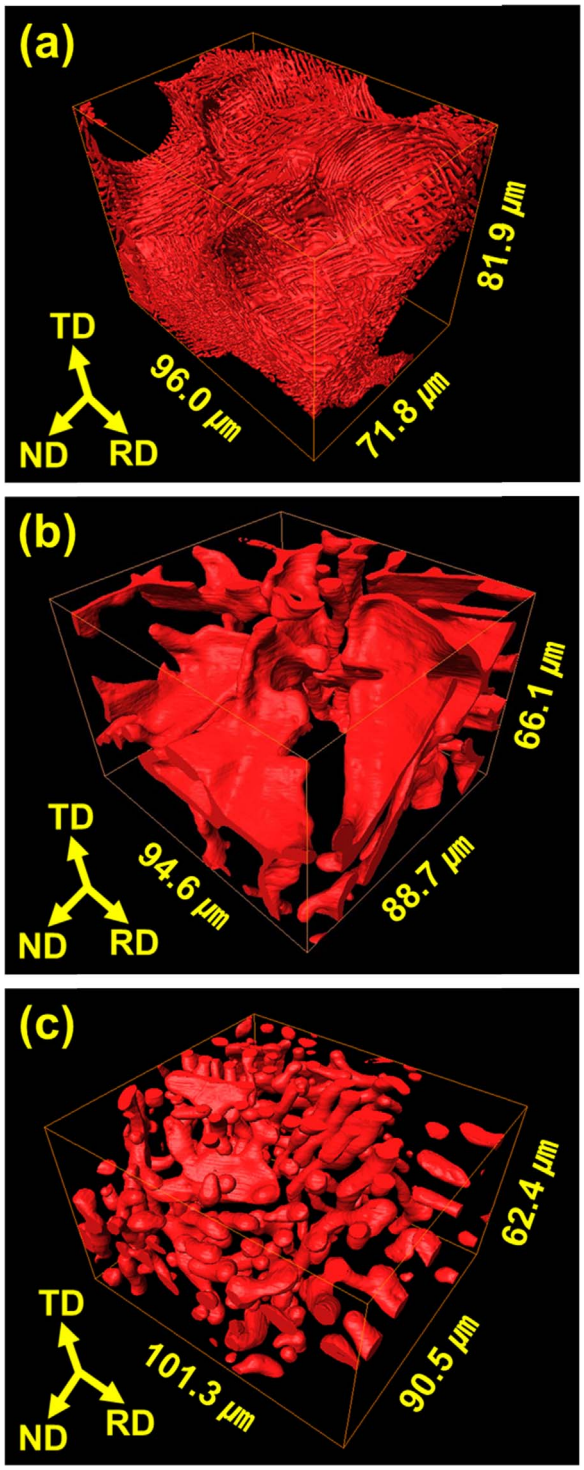

Fig. 6. 3D reconstructed images of the eutectic Mg_2Si in homogenized AlMg5Si2Mn alloys: (a) as-cast (=10.7 vol%), (b) PA treated (=11.8 vol%), and (c) PB treated (=8.4 vol %) samples.

observations clearly show the differences in the interconnectivity of the Mg_2Si of the samples, as displayed in Table 2. Interconnectivity is defined as the fraction of the volume of the largest Mg_2Si with respect to the total volume of Mg_2Si in the analyzed volume [19]. It was confirmed that the PB treatment remarkably reduced the interconnectivity of Mg_2Si particles.

The optical micrographs of the slab after cold rolling during the PB homogenization method are shown in Fig. 7. The eutectic Mg_2Si fibers were severely cracked by cold rolling prior to heating. In spite of the hard eutectic Mg_2Si phases, the ductile α(Al) matrix is capable of accommodating the applied plastic strain, so the incompatibility between the matrix and particles results in the formation of geometrically necessary dislocations (GNDs) [20,21]. This high density of dislocations leads to a highly localized strain in the vicinity of their interface, and results in the mechanical fragmentation of the eutectic Mg_2Si particles during cold rolling prior to homogenization. In addition, it can be observed that the particle cracking considerably depends on the direction of the applied load during cold rolling prior to homogenization. The Mg_2Si particles observed in the RD section were randomly cracked without preferred direction, as shown in Fig. 7(a). In the TD section (Fig. 7(b)) and ND section (Fig. 7(c)), the most of cracks appear to be aligned parallel to the ND and TD, i.e., they are perpendicular to the direction of induced tensile stress. It is because the slab was deformed in compression along the ND and in tension

Table 2
Volumes and interconnectivity of Mg_2Si particles of AlMg5Si2Mn alloys in as-cast, PA and PB treated samples.

Sample	Analyzed volume (μm^3)	Total Mg_2Si volume (μm^3)	Largest Mg_2Si volume (μm^3)	Interconnectivity* of Mg_2Si (%)
As-cast	566,784	60,323	52,450	86.9
PA treated	554,646	58,637	45,551	77.7
PB treated	569,842	47,803	3644	7.6

* Defined as fraction of largest to total Mg_2Si volumes.

along the RD during rolling. Once the tensile stress in the RD exceeds the fracture stress of Mg_2Si particles, the cracks can initiate and propagate perpendicular to the RD [22–25].

As previously reported [26], the morphological changes observed for eutectic Mg_2Si in Al-Mg-Si alloys are similar to those of eutectic Si in Al-Si alloys during heat treatment. In brief, the regions of faults in the lamellar eutectic Si break up into relatively smaller fragments, leading to diffusion-controlled spheroidization, and the fragments then become spheroid and coarsened with increasing time [27–29]. From this point of view, the accelerated spheroidization of eutectic Mg_2Si can be understood by the following mechanisms, and the schematic representation shown in Fig. 8.

1. First, the mechanical fragmentation of eutectic Mg_2Si fibers occurs due to applied cold deformation.
2. Second, the regions of faults in the remaining eutectic Mg_2Si fibers break up into fragments, and the artificially cracked planes become spherical, which reduces their surface energy during the initial stages of heat treatment.
3. Finally, these broken particles are spheroidized due to atomic diffusion, and coarsened through the Ostwald ripening [30] mechanism during heat treatment.

In other words, the artificially applied cold deformation causes interfacial instability and/or shape perturbations, which is essential for the initial fragmentation of the Mg_2Si particles. The sharp corners of the broken Mg_2Si particles can easily dissolved into the α(Al) matrix due to their small curvature radius, whereas the planar interface will grow further, to reduce their curvature radius. In addition, the formation of excess vacancies during plastic deformation can contribute to enhanced atomic diffusion, by increasing the number of sites for diffusion.

The primary α(Al) dendrites are first formed from the AlMg5Si2Mn alloy melt, and then surrounded by the co-solidified lamellar structure of the eutectic α(Al)+Mg_2Si. The lamellar morphology of the eutectic phases associated with the casting structure dramatically reduces their mechanical properties [16,31,32]. Accordingly, numerous studies have been carried out to modify eutectic Mg_2Si particles in an effort to improve the mechanical properties of these kinds of alloys. Most of these approaches can be categorized into two major groups. The first

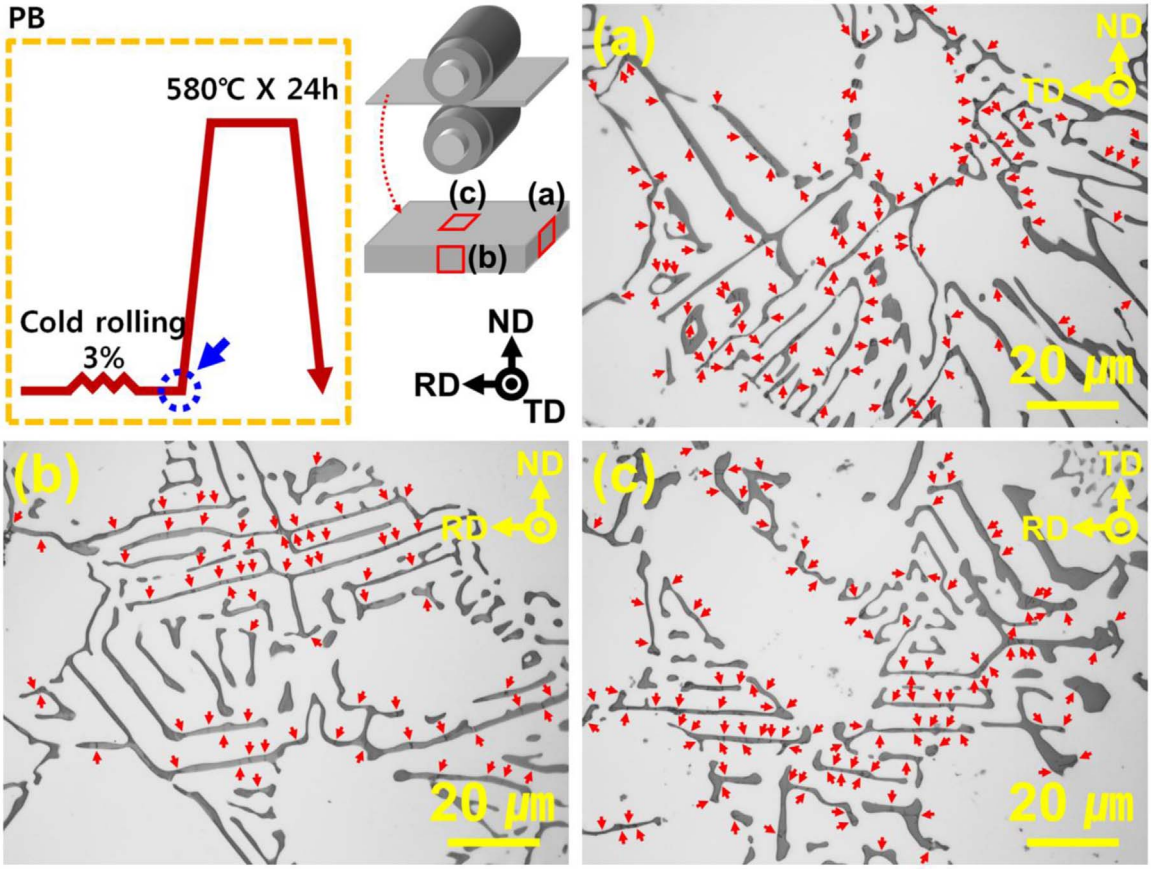

Fig. 7. Microstructures of AlMg5Si2Mn alloy slab after being cold rolled, showing dimensional reductions of 3% prior to homogenization (PB treated sample): (a) RD section, (b) TD section, and (c) ND section.

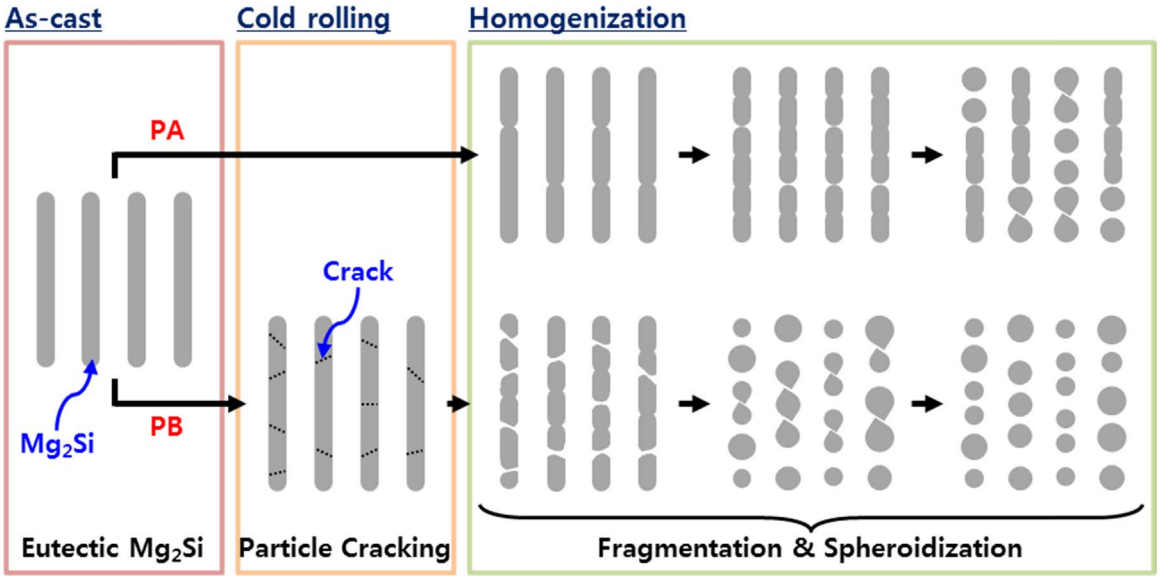

Fig. 8. Schematic representation of the effect of homogenization treatment on the spheroidization sequences of eutectic Mg_2Si in PA and PB treated samples.

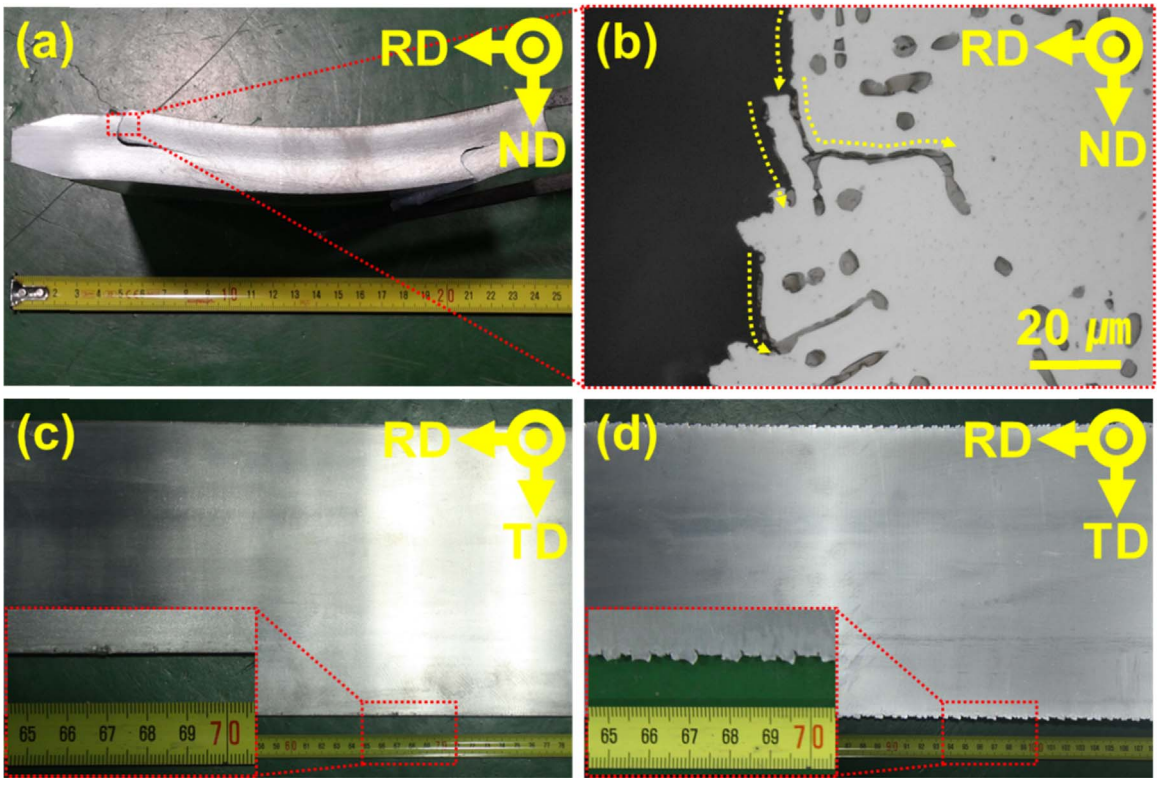

Fig. 9. (a) PA treated slab after hot rolling, (b) optical micrograph of cracked part, marked by the dashed rectangle in (a), (c) PB treated slab after hot rolling, and (d) PB treated slab after hot and subsequent cold rolling.

method uses a long heat treatment time at high temperature [7,33], which is both time and energy consuming. The second method, chemical modification through the addition of several modifying elements such as Sr, Ca, Na, Ti, Li and P [12,20,34–38], can increase porosity as well as cause environmental problems. Here, we suggest that slight cold deformation prior to homogenization is a more feasible method for modifying eutectic Mg_2Si particles.

We tried hot rolling the PA treated and PB treated slabs, and the hot rolling behavior can be seen in Fig. 9. Surface cracks were generated at the initial stage of the hot rolling and propagated to the center in the PA treated slab, as can be observed in Fig. 9(a). In order to identify the failure modes, the crack growth characteristics were investigated and are shown in Fig. 9(b). It can be seen that the cracks initiate from the brittle Mg_2Si particles at the slab surface and have propagated mainly along the longish-fiber-like eutectic Mg_2Si particles, where several spheroidized eutectic Mg_2Si particles seem to be fractured. On the other hand, the PB treated slab did not show any visible cracks during hot and subsequent cold rolling up to 96% total reduction in thickness, as shown in Fig. 9(c) and (d), respectively. This indicates that the slight cold rolling prior to homogenization may be an effective method to

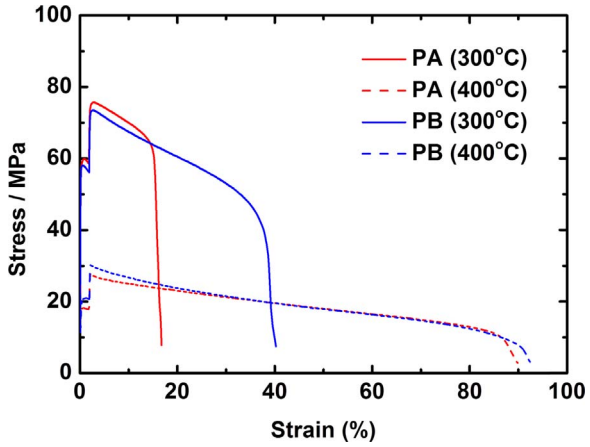

Fig. 10. Stress-strain curves of PA and PB treated AlMg5Si2Mn alloy slabs at 300 and 400 °C.

improve the hot workability of AlMg5Si2Mn alloys.

The stress-strain curves of PA and PB treated slabs at the vicinity of hot rolling temperatures (300 and 400 °C) are presented in Fig. 10. The elongation of both PA and PB treated samples was similar at 400 °C, but PA treated sample exhibited apparently reduced elongation compared to PB treated sample at 300 °C. Difference in elongation at 300 °C can be related with the difference in hot workability of these two samples. During hot rolling, the slabs were heated at 400 °C, but the actual rolling temperature will be quite lower. The surface area of the slabs might be cooled down very quickly due to heat transfer between the rolling mills and the slabs. In the PA treated sample, the high interconnectivity of Mg_2Si particles could hinder dislocation movement, leading to the dislocation pile-up and the increased dislocation density between the matrix and particles. Cracks can initiate at the brittle Mg_2Si particles and propagate mainly along the longish-fiber-like eutectic Mg_2Si particles, as previously shown in Fig. 9.

3.2. Microstructure and mechanical properties of the rolled sheets

The optical micrographs of the sheets that were fabricated by rolling PB treated slab and further solution heat treatment are shown in Fig. 11. The solution heat treatment was carried out at 580 °C to change the Mg_2Si morphology and the grain structure of the matrix. The Mg_2Si particles in the as-rolled sheets had a relatively irregular faceted plane, as shown in Fig. 11(a). The elongated grain structure was developed by cold rolling, as shown in Fig. 11(e). The morphology of the Mg_2Si particles was gradually changed from irregular faceted to a more rounded and/or spherical shape after solution treatment at increasing time, as shown in Fig. 11(b)–(d). The growth of Mg_2Si particle was negligibly small. Equiaxial grains were formed by solution heat treatment, and the grain size gradually increased with increasing heat treatment time, as shown in Fig. 11(e)–(h).

The average diameter and aspect ratio of the Mg_2Si particles obtained with various solution heat treatment times are shown in Fig. 12(a). The average diameters did not significantly change, but the aspect ratio was slightly decreased by the heat treatment. The average grain diameter gradually increased with increasing solution treatment time, as shown in Fig. 12(b). The most suitable homogenization condition for Mg_2Si particle morphology and grain growth was determined to be 580 °C for 1 h.

The mechanical properties of the cast and the PB treated and rolled sheets are summarized in Table 3. It was not possible to obtain samples for testing from the PA treated slab due to severe cracks, as shown in Fig. 9, and thus those obtained from the as-cast slab were used for comparison (designated “F” in Table 3). It can be seen that the mechanical properties of the PB treated samples were significantly improved, compared to those of the as-cast samples. Both the yield and tensile strength were increased by cold rolling prior to homogenization, to 6.7 and 38.0 MPa, respectively, for the T4 heat treatment condition. In particular, the elongation to failure was 340% higher than that of the as-cast sample for this condition. After the T6 heat treatment, the PB treated samples still retained higher mechanical properties than those of the as-cast samples. The improved mechanical properties of the PB treated and rolled sheets may be attributed to several reasons, as follows.

(1) The morphological change of the eutectic Mg_2Si phase in the α(Al) matrix from lamellar to spherical can help to not only reduce stress concentration, but reduce crack initiation as well [39,40]. As seen, the thermomechanically treated AlMg5Si2Mn alloy showed better mechanical properties than the as-cast sample, due to the spheroidization of Mg_2Si. Uniform distribution of the spheroid Mg_2Si particles was more effective in strengthening the aluminum alloys than the non-uniform distribution of longish, irregular, acicular (often needle-like), lamellar-type particles at the dendritic boundaries [20,31,32]. In other words, the spheroidization of the Mg_2Si particles can eliminate the particles’ facets, thereby reducing the stress concentration, and enhancing the alloy ductility.

(2) In case of the AlMg5Si2Mn alloy containing Mg and Si as major elemental additions, β-Mg_2Si can be precipitated from a supersaturated

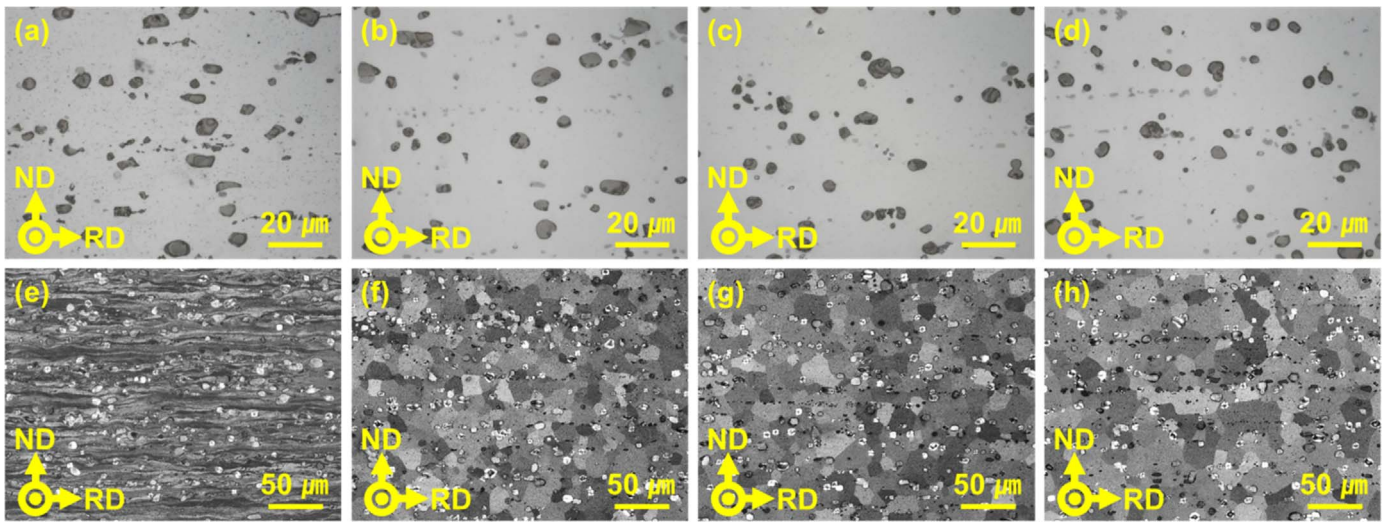

Fig. 11. Microstructural changes of Mg_2Si particles ((a)–(d)) and crystal grains ((e)–(h)) during solution heat treatment at 580 °C for 0 h (as-rolled, (a) and (e)), 0.5 h ((b) and (f)), 4 h ((c) and (g)), and 8 h ((d) and (h)).

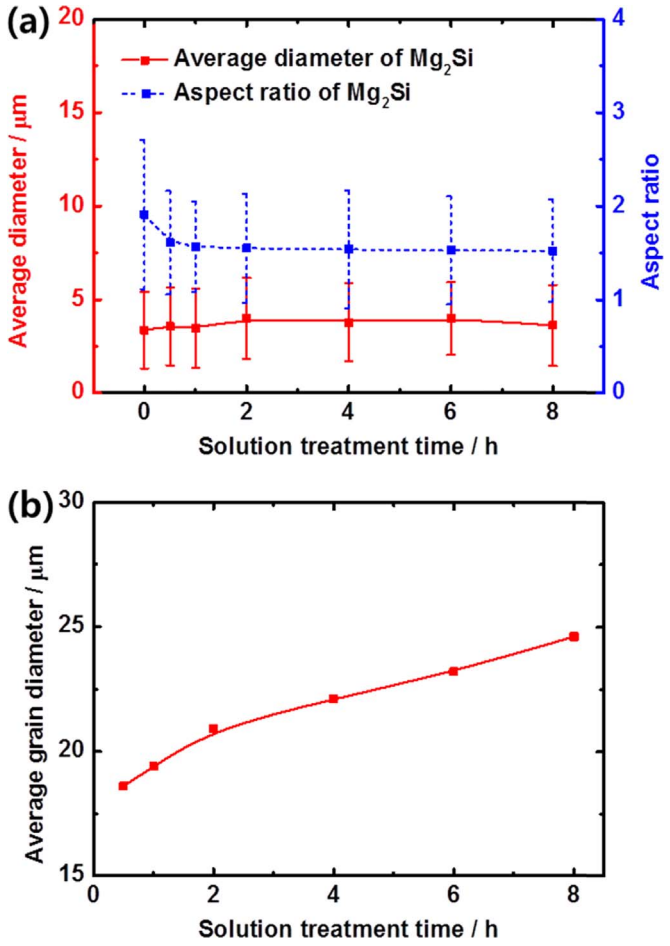

Fig. 12. (a) Morphologies of Mg_2Si particles, and (b) grain size of matrix, as a function of solution treatment time at 580 °C.

Table 3
Tensile properties of the cast slab and the PB treated and rolled sheets.

Sample	Tensile strength (MPa)	Yield strength (MPa)	Elongation (%)
Cast slab (F)	204.9	90.2	6.1
Cast slab (T6)	222.6	153.7	3.2
Rolled sheet* (T4)	242.9	96.9	20.9
Rolled sheet* (T6)	248.6	179.6	11.5

* PB treated, hot rolled, cold rolled and heat treated sheets.

solid solution in the α(Al) matrix after an artificial aging treatment [31,41]. The matrix can be strengthened by the precipitation of the intermetallic compound β-Mg_2Si. Note that the precipitates may be present in both the as-cast and PB treated sheets. However, for the PB treated sheets, the finely dispersed Mg_2Si particles cause an increase in the specific surface area, and as a result, the Mg and Si atoms can be easily supersaturated during solution heat treatment.

(3) Average grain size was significantly reduced after the thermomechanical treatment, as shown in Fig. 4(a) and Fig. 11(f)–(h). This grain refinement can create a high volumetric density of grain boundaries which impede dislocation movement and dislocation propagation to adjacent grains, thereby strengthening the materials [42–44]. In addition, elongation can also be increased with reduced grain size, by homogeneous deformation for the given total strain [45].

(4) Casting defects such as gas porosity and/or shrinkage voids, which lead to the deterioration of mechanical properties (especially related to ductility) due to stress concentration [46,47], can subsequently be eliminated by thermomechanical treatment.

Consequently, the mechanical properties of the AlMg5Si2Mn alloy were significantly improved by the newly designed thermomechanical treatment process, confirming the potential of applying casting aluminum alloys to wrought products.

4. Conclusion

In this study, the microstructure and mechanical properties of AlMg5Si2Mn alloys were investigated following a modified homogenization treatment, to evaluate the effect of the treatment on the potential application of casting aluminum alloys in wrought aluminum alloy products. The results can be summarized as follows:

(1) The slight cold rolling prior to homogenization improved the hot workability of the AlMg5SiMn alloy, compared to a conventional homogenization process, by accelerating the spheroidization of eutectic Mg_2Si particles. The main reason for this improvement was the mechanical fragmentation of the eutectic Mg_2Si particles during cold rolling.
(2) The mechanical properties of the AlMg5Si2Mn sheets were significantly increased by the thermomechanical treatment. Both the yield and tensile strength were improved by the combination of homogeneously distributed Mg_2Si particles and fine grain size. Ductility was also increased by the proposed treatment, which reduced grain size and removed casting defects.
(3) It is concluded that cold rolling prior to the homogenization process may be an effective method of enhancing the workability and mechanical properties of aluminum casting alloys, without the need for long time heat treatment and/or alloy modification.

Acknowledgments

This research was supported by the Strategic Core Materials Technology Development Program (No. 10050625) funded by the Ministry of Trade, Industry and Energy (MOTIE, South Korea).

References

[1] J. Hirsch, T. Al-Samman, Acta Mater. 61 (2013) 818–843.
[2] H. Zhong, P.A. Rometsch, L. Cao, Y. Estrin, Mater. Sci. Eng. A 651 (2016) 688–697.
[3] X.L. Huang, A.E. Badawy, M. Arambewela, R. Ford, M.A. Barlaz, T. Tolaymat, J. Hazard. Mater. 273 (2014) 192–199.
[4] ASM, ASM Handbook: Properties and Selection: Nonferrous Alloys and Special-Purpose Materials, 10th ed., ASM International, Materials Park, OH, 1990.
[5] Z. Hu, Mater. Manuf. Process. 31 (2016) 787–793.
[6] Z. Hu, L. Wan, S. Wu, H. Wu, X. Liu, Mater. Des. 46 (2013) 451–456.
[7] A. Malekan, M. Emamy, J. Rassizadehghani, A.R. Emami, Mater. Des. 32 (2011) 2701–2709.
[8] M. Emamy, A.R. Emami, K. Tavighi, Mater. Sci. Eng. A 651 (2013) 36–44.
[9] Z. Li, C. Li, Y. Liu, L. Yu, Q. Guo, H. Li, J. Alloy. Compd. 663 (2016) 16–19.
[10] M. Tebib, A.M. Samuel, F. Ajersch, X.-G. Chen, Mater. Charact. 89 (2014) 112–123.
[11] Q.D. Qin, Y.G. Zhao, C. Liu, P.J. Cong, W. Zhou, J. Alloy. Compd. 454 (2008) 142–146.
[12] Q.D. Qin, Y.G. Zhao, W. Zhou, P.J. Cong, Mater. Sci. Eng. A 447 (2007) 186–191.
[13] Y.G. Zhao, Q.D. Qin, W. Zhou, Y.H. Liang, J. Alloy. Compd. 389 (2005) L1–L4.
[14] J. Zhang, Z. Fan, Y.Q. Wang, B.L. Zhou, Mater. Sci. Eng. A 281 (2000) 104–112.
[15] F. Liu, F. Yu, D. Zhao, L. Zuo, Mater. Sci. Eng. A 528 (2011) 3786–3790.
[16] R. Franke, D. Dragulin, A. Zovi, F. Casarotto, Metall. Ital. 5 (2007) 21–26.
[17] J.E. Spowart, H.E. Mullens, B.T. Puchala, J. Miner. Metals Mater. Soc. 55 (2003) 35–37.
[18] D. Shimosaka, S. Kumai, F. Casarotto, S. Watanabe, Mater. Trans. 52 (2011) 920–927.
[19] Z. Asghar, G. Requena, E. Boller, Acta Mater. 59 (2011) 6420–6432.
[20] A.H. Shafieizad, A. Zarei-Hanzaki, H.R. Abedi, K.J. Al-Fadhalah, Mater. Sci. Eng. A 644 (2015) 310–317.
[21] M. Vogelsang, R.J. Arsenault, R.M. Fisher, Metall. Trans. A 17 (1986) 379–389.
[22] H. Agarwal, A.M. Gokhale, S. Graham, M.F. Horstemeyer, Metall. Mater. Trans. A 33 (2002) 3443–3448.
[23] S.G. Lee, Y. Mao, A.M. Gokhale, J. Harris, M.F. Horstemeyer, Mater. Charact. 60 (2009) 964–970.
[24] S.G. Lee, Met. Mater. Int. 15 (2009) 591–596.
[25] S.K. Shaha, F. Czerwinski, W. Kasprzak, D.L. Chen, Mater. Des. 59 (2014)

352–358.
[26] D. Tolnai, G. Requena, P. Cloetens, J. Lendvai, H.P. Degischer, Mater. Sci. Eng. A 585 (2013) 480–487.
[27] M. Haghshenas, A. Zarei-Hanzaki, S.M. Fatemi-Varzaneh, Mater. Sci. Eng. A 480 (2008) 68–74.
[28] A.M.A. Mohamed, A.M. Samuel, F.H. Samuel, H.W. Doty, Mater. Des. 30 (2009) 3943–3957.
[29] B. Li, H. Wang, J. Jie, Z. Wei, Mater. Des. 32 (2011) 1617–1622.
[30] W. Ostwald, Z. Phys. Chem. 22 (1897) 289–330.
[31] E. Georgatis, A. Lekatou, A.E. Karantzalis, H. Petropoulos, S. Katsamakis, A. Poulia, J. Mater. Eng. Perform. 22 (2013) 729–741.
[32] L. Bian, W. Liang, G. Xie, W. Zhang, J. Xue, Mater. Sci. Eng. A 528 (2011) 3463–3467.
[33] E. Sjölander, S. Seifeddine, J. Mater. Process. Technol. 210 (2010) 1249–1259.
[34] L. Hengcheng, S. Yu, S. Guoxiong, Mater. Sci. Eng. A 358 (2003) 164–170.
[35] S.S. Sreeja Kumari, R.M. Pillai, B.C. Pai, J. Alloy. Compd. 460 (2008) 472–477.
[36] M. Emamy, R. Khorshidi, A.H. Raouf, Mater. Sci. Eng. A 528 (2011) 4337–4342.
[37] N. Soltani, A. Bahrami, M.I. Pech-Canul, Metall. Mater. Trans. A 44 (2013) 4366–4373.
[38] R. Hadian, M. Emamy, N. Varahram, N. Nemati, Mater. Sci. Eng. A 490 (2008) 250–257.
[39] J.W. Yeh, W.P. Liu, Metall. Mater. Trans. A 27 (1996) 3558–3568.
[40] N. Nasiri, M. Emamy, A. Malekan, Mater. Des. 37 (2012) 215–222.
[41] L. Pedersen, L. Arnberg, Metall. Mater. Trans. A 32 (2001) 525–532.
[42] E.O. Hall, Proc. Phys. Soc. B64 (1951) 747–753.
[43] N.J. Petch, J. Iron Steel Inst. 174 (1953) 25–28.
[44] K. Ma, H. Wen, T. Hu, T.D. Topping, D. Isheim, D.N. Seidman, E.J. Lavernia, J.M. Schoenung, Acta Mater. 62 (2014) 141–155.
[45] T.M. Yue, H.U. Ha, N.J. Musson, J. Mater. Sci. 30 (1995) 2277–2283.
[46] C.H. Cáceres, B.I. Selling, Mater. Sci. Eng. A 220 (1996) 109–116.
[47] J.Z. Yi, Y.X. Gao, P.D. Lee, H.M. Flower, T.C. Lindley, Metall. Mater. Trans. A 34 (2003) 1879–1890.